ELSEVIER

NeuroImage

www.elsevier.com/locate/ynimg
NeuroImage 23 (2004) 425–433

Rapid Communication

Structural brain variation and general intelligence

Richard J. Haier,[a,*] Rex E. Jung,[b] Ronald A. Yeo,[c] Kevin Head,[a] and Michael T. Alkire[d]

[a] *Department of Pediatrics, University of California, Irvine, CA 92697-5000, USA*
[b] *Department of Neurology, and the MIND Institute, University of New Mexico, Albuquerque, NM 87131, USA*
[c] *Department of Psychology, University of New Mexico, Albuquerque, NM 87131, USA*
[d] *Department of Anesthesiology, University of California Irvine Medical Center, Orange, CA 92868-1350, USA*

Received 10 March 2004; revised 14 April 2004; accepted 22 April 2004
Available online 15 July 2004

Total brain volume accounts for about 16% of the variance in general intelligence scores (IQ), but how volumes of specific regions-of-interest (ROIs) relate to IQ is not known. We used voxel-based morphometry (VBM) in two independent samples to identify substantial gray matter (GM) correlates of IQ. Based on statistical conjunction of both samples ($N = 47$; $P < 0.05$ corrected for multiple comparisons), more gray matter is associated with higher IQ in discrete Brodmann areas (BA) including frontal (BA 10, 46, 9), temporal (BA 21, 37, 22, 42), parietal (BA 43 and 3), and occipital (BA 19) lobes and near BA 39 for white matter (WM). These results underscore the distributed neural basis of intelligence and suggest a developmental course for volume–IQ relationships in adulthood.
© 2004 Elsevier Inc. All rights reserved.

Keywords: IQ; Brain volume; Morphometry

Introduction

Correlations between regional brain function and performance on mental tests associated with a general intelligence factor (*g*) as defined originally by Spearman (1904) have been demonstrated many times in normal subjects (Duncan et al., 2000; Gray et al., 2003; Haier et al., 1988; Haier and Benbow, 1995; Parks et al., 1988; Prabhakaran et al., 1997). Most of these studies show that good test performance recruits areas distributed throughout the brain, although a case has been made that activation within areas of the frontal lobes is the primary source of differences in *g*-loaded test performance (Duncan et al., 2000). There is evidence that deactivation within some brain areas, including frontal lobes, is associated with better mental task performance (Haier et al., 1988, 1992a; Parks et al., 1988), especially in subjects with higher intelligence test scores (Haier et al., 1992b). Even when a passive task with no inherent problem solving is used, subjects with higher intelligence scores show more activation in posterior information processing areas than subjects with lower scores (Boivin et al., 1992; Haier et al., 2003b).

Functional brain imaging studies always must be interpreted to take account of the specific task demands of the mental task used during the imaging protocol. This makes inconsistencies among study results difficult to reconcile given the wide variety of tasks used. To the extent that individual differences in general intelligence have a structural component, examining structural correlates of intelligence would eliminate any task-related influences from consideration. For this reason, structural imaging of regional gray and white matter volumes would provide unique information about the distribution of brain areas related to general intelligence.

For example, total brain volume assessed by MRI in many studies has been shown to correlate about $r = 0.40$, with intelligence scores and total gray and white matter volumes also show small correlations with IQ (Gignac et al., 2003), but attempts to relate volume of specific brain areas to test scores have been mostly unsuccessful (Flashman et al., 1997; MacLullich et al., 2002). Until now, such attempts have used various region-of-interest (ROI) methods that are difficult to reliably apply to many brain gyri when outlined by hand and often do not conform well to the extensive individual differences among subjects in brain size and morphology when applied stereotactically. A recent methodological advance is optimized voxel-based morphometry (VBM), which uses algorithms to segment gray matter (GM) and white matter (WM) from structural MRIs (Ashburner and Friston, 2000; Good et al., 2001). VBM has been validated extensively (Ashburner and Friston, 2001; Good et al., 2002) and it has been used, for example, to characterize gray and white matter volume changes in aging (Good et al., 2001), dementia (Good et al., 2002), and Down syndrome (White et al., 2003).

Materials and methods

Subjects

We tested two samples and used a statistical conjunction approach (Price and Friston, 1997) to show where correlations between IQ and gray or white matter were common to both samples. The first sample was 23 normal volunteers (14 women and 9 men;

* Corresponding author. Department of Pediatrics, University of California Irvine, Medical Science I, B140, Irvine, CA 92697. Fax: +1-949-824-9059.
E-mail address: rjhaier@uci.edu (R.J. Haier).
Available online on ScienceDirect (www.sciencedirect.com.)

1053-8119/$ - see front matter © 2004 Elsevier Inc. All rights reserved.
doi:10.1016/j.neuroimage.2004.04.025

mean age = 27, SD = 5.9, range = 18–37) recruited from the University of New Mexico (UNM). Sample 1 MRIs were obtained with a 1.5-T scanner, head coil, and software (Signa 5.4; General Electric Medical Systems, Waukesha, WI). A T1 sagittal localizer sequence (TE = 6.9 ms, TR = 200 ms, FOV = 24 × 24 cm^2, five slices, thickness = 5 mm, spacing = 2.5 mm, matrix = 256 × 128) was acquired, followed by a T1-weighted axial series (fast RF spoiled gradient-recalled, TE = 6.9 ms, TR = 17.7 ms, flip angle = 25°, matrix = 256 × 192, 120 slices, thickness = 1.5 mm) to give full brain coverage.

The second sample was 24 normal volunteers (13 men and 11 women, mean age = 59, SD = 15.9, range 37–84) recruited at the University of California (UCI), Irvine, as middle-aged and older normal controls for an imaging study of dementia in Down syndrome and Alzheimer's disease (Haier et al., 2003a). Sample 2 MRIs were obtained with a 1.5-T clinical Phillips Eclipse scanner (Philips Medical Systems, N.A., Bothell, WA). We used T1-weighted, volumetric SPGR MRI scans (FOV = 24 cm, flip angle = 40, TR = 24, TE = 5). The images consisted of 120 contiguous 1.2-mm thick axial slices, each with an in-plane image matrix of 256 × 256 image elements. All images in both samples were visually inspected to ensure image quality.

Intelligence testing

To assess general intelligence, subjects were tested with the Wechsler Adult Intelligence Scale (WAIS). The WAIS battery (Wechsler, 1981) consists of 11 diverse subtests, which tap a variety of verbal and nonverbal mental abilities that contribute to general intelligence. The WAIS Full Scale IQ (FSIQ) score is based on performance of all 11 subtests (according to age based norms). Factor analytic studies (Jensen, 1980) show that each subtest loads on the *g* factor and the FSIQ score loads the highest (about 0.90 or 81% of the variance in *g*). For this reason, FSIQ is considered one of the best indexes of individual differences in general intelligence. For sample 1 (UMN), the FSIQ was 116 (SD = 14.7) and the range was 90–155. For sample 2 (UCI), the mean FSIQ was 116 (SD = 14.2) and the range was 90–142.

Voxel-based morphometry

We applied VBM to identify brain areas where GM and WM volumes are correlated to FSIQ to test whether any such areas are clustered in frontal lobes or distributed throughout the brain. We used Statistical Parametric Mapping software (SPM2; The Wellcome Department of Imaging Neuroscience, University College London) to create a study-specific template and then applied the optimized VBM protocol to each sample separately using the methods of Ashburner and Friston (2000) and Good et al. (2001). To preserve the amount of tissue in any given anatomical region after spatial normalization, the optimal GM and WM partitions were multiplied by the Jacobian determinants of their respective spatial transformation matrix. The reason for performing this modulation step is so that the final VBM statistics will reflect local deviations in the absolute amount (volume) of tissue in different regions of the brain (Ashburner and Friston, 2000). The modulated GM and WM partitions were then smoothed with a 12-mm FWHM isotropic Gaussian kernel to account for slight misalignments of homologous anatomical structures and to ensure statistical validity under parametric assumptions.

Statistical conjunction approach

We specifically tested whether regional gray and white matter volumes were correlated with FSIQ scores treating any effects of age, sex, and handedness (three cases in the UNM sample were left handed) as nuisance variables in the SPM2 design matrix. After computing the correlation analyses for each sample separately, we

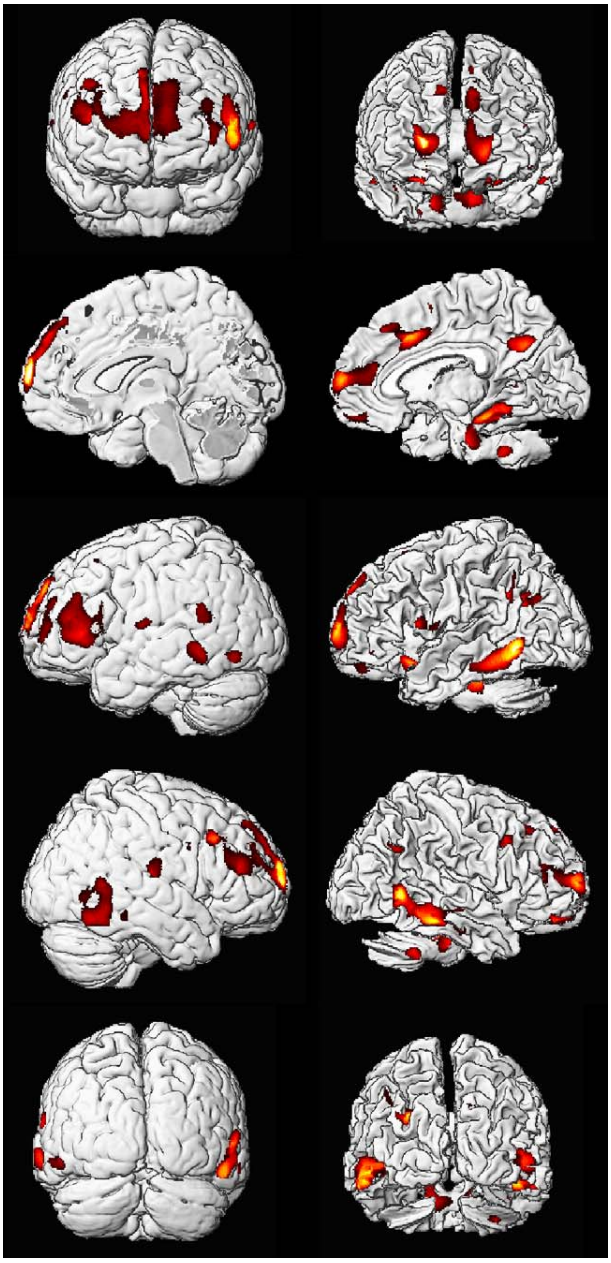

Fig. 1. Correlations between gray and white matter and FSIQ conjuncted across both samples. Based on statistical conjunction, correlations between gray matter and FSIQ are shown in the left column on gray matter templates; white matter correlations to FSIQ are shown in the right column on a white matter template. Top row shows frontal view, second row shows medial sagittal view, next rows show left and right lateral views, and bottom row shows occipital view. Anatomical locations, atlas coordinates, and cluster sizes are listed in Table 1.

Table 1
Localization of conjunction correlations from UNM and UCI between gray and white matter with FSIQ ($P \leq 0.001$)

Brain area (and/or nearest gray matter)	Cluster size	x	y	z	t	r^2
Gray matter correlations with FSIQ						
Right medial frontal gyrus, BA 10*	6846	2	66	6	4.65	0.35
Right medial frontal gyrus, BA 10*		−8	63	17	4.38	0.32
Right superior frontal gyrus, BA 9*		4	56	31	4.29	0.31
Left middle frontal gyrus, BA 46*	3464	−50	39	17	4.32	0.31
Left inferior frontal gyrus, BA 45*		−51	31	5	4.13	0.29
Left middle frontal gyrus, BA 46*		−50	35	24	3.92	0.27
Left middle temporal gyrus, BA 21*	692	−66	−45	−4	3.93	0.27
Right frontal precentral gyrus, BA 9*	705	37	23	34	3.86	0.27
Right middle frontal gyrus, BA 9*		49	32	32	3.22	0.20
Right temporal inferior gyrus, BA 37*	2294	55	−60	−10	3.84	0.26
Right temporal middle gyrus, BA 37*		57	−51	−8	3.65	0.25
Right temporal middle gyrus, BA 21*		61	−48	−3	3.51	0.23
Left middle frontal gyrus, BA 10*	524	−40	56	3	3.75	0.26
Left superior frontal gyrus, BA 10*		−36	51	23	3.65	0.25
Left middle frontal gyrus, BA 10*		−41	53	9	3.51	0.23
Left middle occipital gyrus, BA 19*	345	−54	−68	−5	3.66	0.25
Left temporal superior gyrus, BA 22*	426	−63	−48	19	3.61	0.24
Left parietal supramarginal gyrus, BA 40*		−66	−45	26	3.42	0.22
Left temporal transverse gyrus, BA 42*	218	−62	−9	12	3.47	0.23
Right parietal postcentral gyrus, BA 43*	385	64	−17	15	3.46	0.23
Right parietal postcentral gyrus, BA 3*		61	−15	23	3.36	0.22
Right temporal middle gyrus, BA 21*	45	65	−35	−10	3.30	0.21
Left frontal superior gyrus, BA 8*	13	−41	23	50	3.28	0.21
Right frontal inferior gyrus, BA 9*	20	58	7	30	3.28	0.21
White matter correlations with FSIQ						
Right temporal middle gyrus, BA 39*	4457	51	−54	5	3.48	0.23
Right temporal fusiform gyrus, BA 37		50	−37	−10	3.24	0.20
Right middle temporal gyrus, BA 21		55	−33	−3	2.51	0.13
Left temporal middle gyrus, BA 20	4325	−52	−40	−9	3.38	0.22
Left temporal inferior gyrus, BA 19		−44	−53	−1	3.14	0.19
Left temporal middle gyrus, BA 37		−52	−53	2	2.70	0.15
Left frontal superior gyrus, BA 10	1839	−18	60	1	4.55	0.34
Left frontal medial gyrus, BA 10		−7	63	8	3.92	0.27
Left frontal medial gyrus, BA 10		−8	62	21	3.47	0.23
Left frontal inferior gyrus, BA 47	813	−23	13	−13	2.98	0.18
Right frontal middle gyrus, BA 10	2126	29	59	8	2.93	0.17
Right frontal superior gyrus, BA 10		21	62	6	2.85	0.17
Right frontal medial gyrus, BA 10		24	44	10	2.36	0.12
Left parietal precuneus, BA 7	2675	−23	−60	30	2.79	0.16
Left parietal precuneus, BA 7		−15	−52	24	2.37	0.12
Right parietal precuneus, BA 31	1288	18	−58	35	2.79	0.16
Right limbic cingulate gyrus, BA 24	1819	13	15	32	2.75	0.16
Right limbic cingulate gyrus, BA 32		13	9	36	2.30	0.11
Right frontal medial gyrus, BA 8		11	31	39	2.24	0.11
Left frontal superior gyrus, BA 9	582	−10	52	35	2.67	0.15
Left frontal superior gyrus, BA 9		−9	58	32	2.17	0.10
Right limbic, parahippocampus, BA 35	726	17	−26	−21	2.55	0.14
Right limbic, parahippocampus, BA 35		19	−30	−14	2.36	0.12
Left limbic, parahippocampus, BA 35	1580	−14	−28	−19	2.46	0.13
Left brainstem, pons		−4	−31	−22	2.27	0.11
Left brainstem, midbrain substania nigra		−11	−27	−11	2.21	0.11
Right frontal superior gyrus, BA 11	324	29	49	−15	2.41	0.12
Right frontal superior gyrus, BA 11		24	56	−15	2.11	0.10
Left sublobar, insula, BA 13	245	−43	8	12	2.40	0.12
Right cerebellum, anterior lobe	406	30	−46	−30	2.36	0.12
Right frontal superior gyrus, BA 6	31	3	5	54	2.20	0.11
Left frontal superior gyrus, BA 11	140	−20	47	−17	2.20	0.11
Left frontal precentral gyrus, BA 6	60	−49	−1	11	2.18	0.10
Right temporal, subgyral, BA 20	89	42	−16	−17	2.17	0.10
Left frontal superior gyrus, BA 6	58	−9	20	53	2.14	0.10

x, y, and z coordinates are in Talairach atlas space.
* $P < 0.05$ corrected for multiple comparisons.

used the conjunction approach (Price and Friston, 1997) to show where gray matter (and white matter) correlations overlapped for the UNM and the UCI samples (i.e., voxels with correlations in common for both samples). This conjunction approach minimizes potential problems associated with combining data from different scanners. The conjunction analysis also has the advantage of maximizing statistical power because all 47 subjects are used in the analysis and it is equivalent to a fixed factor model in SPM. Findings are considered significant at $P < 0.05$ corrected for multiple comparisons; findings at $P \leq 0.001$ uncorrected also are shown for hypothesis generation. R^2 estimates were determined using the formula: $R^2 = t^2 / (df + t^2)$ where $df = 41$ (from the SPM2 conjunction design matrix). Locations of significant clusters (centroids) are converted from Montreal Neurological Institute (MNI) to Talairach atlas (Talairach and Tournoux, 1988) coordinates and reported as closest Brodmann area (BA) where possible. Only clusters of at least 10 voxels are reported.

Results

The conjunction results ($N = 47$; Fig. 1) showed robust positive correlations ($P < 0.05$, corrected for multiple comparisons) between FSIQ and gray matter volumes in Brodmann areas (BA) 10, 46, and 9 in frontal lobes; BA 21, 37, 22, and 42 in temporal lobes; BA 43 and 3 in parietal lobes; and BA 19 in the occipital lobe. The size and

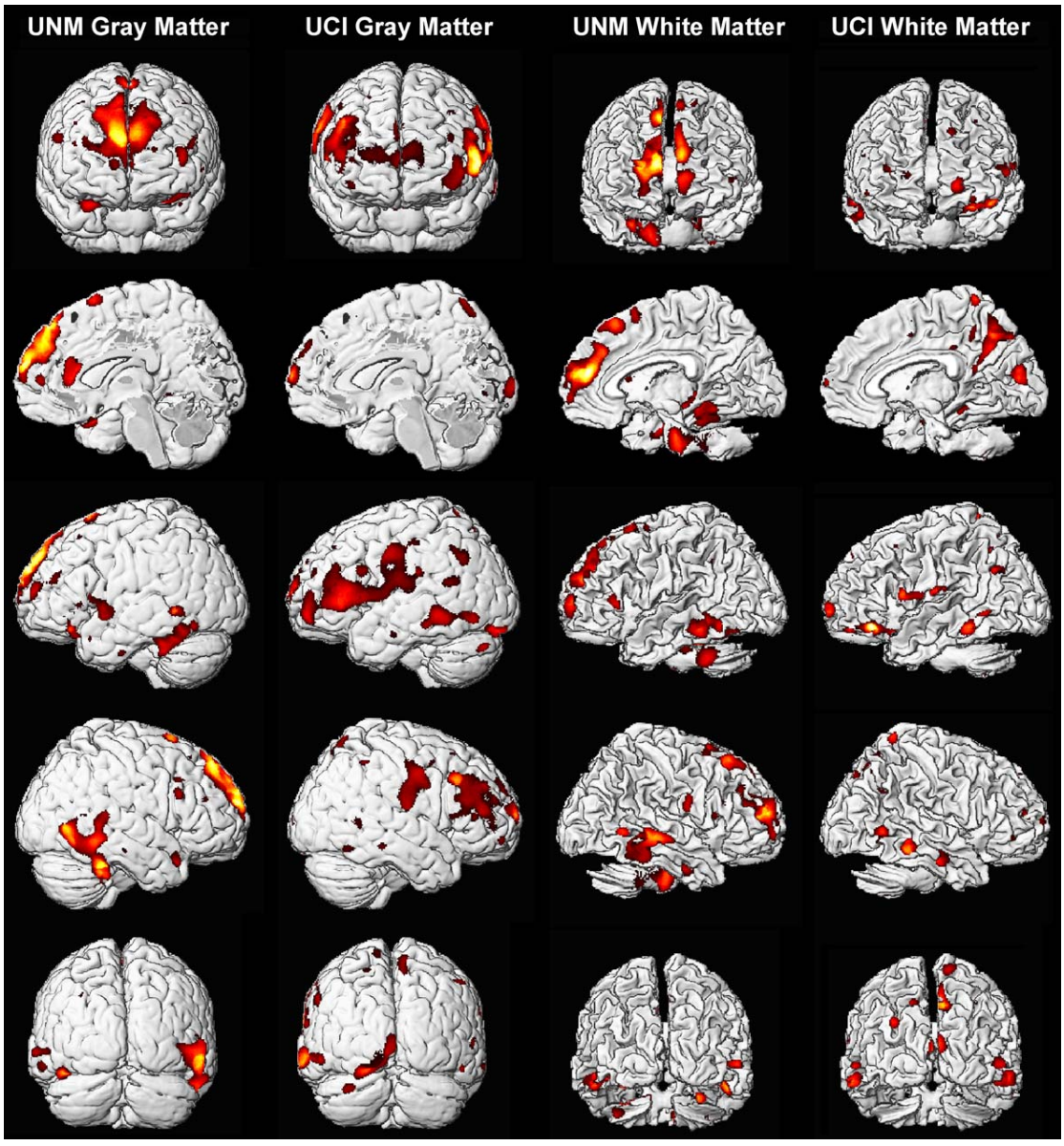

Fig. 2. Correlations between gray and white matter and FSIQ for each sample. Based on separate analyses for each sample, gray matter correlations are shown in the left columns (UNM and UCI, respectively); white matter correlations are shown in the right columns. Top row shows frontal view, second row shows medial sagittal view, next rows show left and right lateral views, and bottom row shows occipital view. Anatomical locations, atlas coordinates, and cluster sizes are listed in Tables 2 (UNM data) and 3 (UCI data).

locations of these areas are shown in Table 1. Similar but less robust correlations with white matter areas ($P \leq 0.001$, uncorrected) were also found (Table 1). Notably, 24 gray matter regions were significant at $P < 0.05$ (corrected), yet only one white matter region was significant at this level. Estimates of FSIQ variability accounted for by the highest correlation for an individual voxel within the significant gray and white matter areas (R^2) are as high as 73% (Table 1). There were no significant negative correlations.

Table 2
Localization of correlations in the UNM sample between gray and white matter with FSIQ ($P \leq 0.001$)

Brain area (and/or nearest gray matter)	Cluster size	x	y	z	t	r^2
Gray matter correlations with FSIQ						
Left temporal fusiform gyrus, BA 37*	3984	−41	−52	−9	6.93	0.73
Left temporal fusiform gyrus, BA 36		−44	−39	−27	4.17	0.49
Left temporal fusiform gyrus, BA 36		−39	−43	−23	4.09	0.48
Left frontal superior gyrus, BA 10	18,470	−7	60	25	6.28	0.69
Right frontal superior gyrus, BA 10		7	63	18	6.03	0.67
Right frontal superior gyrus, BA 8		9	43	54	5.51	0.63
Left frontal superior gyrus, BA 6	1086	0	17	62	5.99	0.67
Right temporal fusiform gyrus, BA 36	10,187	44	−36	−30	5.94	0.66
Right temporal fusiform gyrus, BA 20		51	−40	−27	5.29	0.61
Right temporal middle gyrus, BA 37		57	−62	1	5.18	0.60
Right limbic lobe, anterior cingulate, BA 32	1756	14	30	7	5.36	0.61
Right limbic lobe, anterior cingulate, BA 32		17	31	17	4.42	0.52
Right frontal inferior gyrus, BA 47	962	31	13	−20	5.23	0.60
Left parietal angular gyrus, BA 39	251	−30	−58	34	4.81	0.56
Left limbic lobe, anterior cingulate, BA 32	830	−17	38	16	4.78	0.56
Left frontal middle gyrus, BA 10	602	−40	58	7	4.71	0.55
Left frontal middle gyrus, BA 10		−39	52	13	3.93	0.46
Right frontal superior gyrus, BA 11	121	30	46	−22	4.66	0.55
Left sublobar, insula, BA 13	1517	−43	3	−4	4.63	0.54
Left sublobar, insula, BA 13		−37	13	7	4.00	0.47
Left occipital middle gyrus, BA 19	283	−61	−65	−9	4.48	0.53
Left limbic lobe, cingulate gyrus, BA 23	338	−8	−16	30	4.21	0.50
Left limbic lobe, cingulate gyrus, BA 24		−9	−6	32	3.73	0.44
Right medial frontal gyrus, BA 10	275	13	51	4	4.16	0.49
Left middle temporal gyrus, BA 22	597	−51	−47	1	4.16	0.49
Left frontal inferior gyrus, BA 47	625	−29	24	−19	4.15	0.49
Left frontal inferior gyrus, BA 47		−38	28	−16	4.10	0.48
Left frontal inferior gyrus, BA 47		−25	16	−18	3.91	0.46
Left temporal fusiform gyrus, BA 20	113	−60	−11	−28	4.03	0.47
Right frontal inferior gyrus, BA 9	272	54	21	24	3.97	0.47
Left frontal middle gyrus, BA 46	185	−48	41	20	3.91	0.46
Left frontal middle gyrus, BA 8	17	−42	24	49	3.89	0.46
Right frontal middle gyrus, BA 8	49	38	30	49	3.89	0.46
Left limbic lobe, anterior cingulate, BA 10	69	−12	32	−11	3.85	0.45
Right frontal middle gyrus, BA 10	33	42	40	18	3.83	0.45
Right frontal middle gyrus, BA 9	94	41	21	34	3.79	0.44
Right limbic lobe, parahippocampus, BA 19	29	34	−45	0	3.79	0.44
Left frontal medial gyrus, BA 32	20	−14	14	44	3.75	0.44
Left inferior frontal gyrus, BA 47	35	−54	21	3	3.74	0.44
Left temporal superior gyrus, BA 38	20	−36	13	−20	3.71	0.43
White matter correlations with FSIQ						
Left frontal superior gyrus, BA 9	690	−8	50	21	5.87	0.66
Left frontal medial gyrus, BA 9		−8	44	29	3.84	0.45
Right frontal medial gyrus, BA 10	2234	8	45	14	5.19	0.60
Right frontal medial gyrus, BA 10		18	47	11	4.64	0.54
Right frontal superior, BA 10		25	55	13	4.07	0.48
Right limbic lobe, parahippocampus, amygdala	245	28	−7	−22	5.08	0.59
Right frontal superior gyrus, BA 8	480	11	28	48	5.01	0.58
Right middle temporal gyrus, BA 21	148	59	−52	4	4.95	0.58
Right sublobar, insula, BA 22	1138	44	−27	−1	4.53	0.53
Left temporal middle gyrus, BA 20	205	−50	−37	−10	4.32	0.51
Left medial frontal gyrus, BA 10	345	−10	57	5	4.14	0.49
Left frontal superior gyrus, BA 10		−7	60	−2	3.83	0.45
Right brainstem, pons	146	14	−21	−26	3.97	0.47

x, y, and z coordinates are in Talairach atlas space.
* $P < 0.05$ corrected for multiple comparisons.

The positive correlations between gray and white matter and FSIQ for each sample separately are shown in Fig. 2 and in Tables 2 (UNM) and 3 (UCI); there were no significant negative correlations. Statistical comparisons made directly between the two samples could be difficult to interpret because different MRI scanners were used and the ages were different. An exploratory analysis showed few areas with significant differences between gray and white matter volumes between the samples, and none of these areas overlapped with areas identified in the conjunction analysis.

Another approach to assessing the differences between the samples is shown in Table 4. It shows a comparison between the

Table 3
Localization of correlations in the UCI sample between gray and white matter with FSIQ ($P \leq 0.001$)

Brain area (and/or nearest gray matter)	Cluster size	x	y	z	t	r^2
Gray matter correlations with FSIQ						
Left frontal inferior gyrus, BA 45*	11,086	−55	30	1	7.06	0.70
Left frontal inferior gyrus, BA 46		−56	32	10	5.50	0.59
Left frontal middle gyrus, BA 10		−42	55	−3	5.35	0.58
Left temporal middle gyrus, BA 21	2424	−64	−45	−3	5.15	0.56
Left occipital middle gyrus, BA 19		−53	−67	−3	4.37	0.48
Left temporal middle gyrus, BA 21		−67	−33	−9	3.94	0.43
Right frontal precentral gyrus, BA 9	5177	37	23	34	5.13	0.56
Right frontal middle gyrus, BA 46		53	32	21	4.33	0.47
Right frontal middle gyrus, BA 9		45	25	33	4.31	0.47
Right frontal medial gyrus, BA 10	1869	2	66	6	5.03	0.55
Left frontal medial gyrus, BA 10		−5	65	11	4.43	0.48
Right frontal superior gyrus, BA 10		22	66	11	4.27	0.46
Right frontal precentral gyrus, BA 6	3096	60	−7	41	4.83	0.53
Right frontal precentral gyrus, BA 6		65	−10	32	4.23	0.46
Right parietal postcentral gyrus, BA 43		64	−13	20	4.18	0.45
Left lingual gyrus	4378	−11	−77	1	4.72	0.51
Left occipital fusiform gyrus, BA 18		−21	−87	−12	4.18	0.45
Left occipital cuneus, BA 18		0	−96	6	4.01	0.43
Right parietal precuneus, BA 7	433	9	−61	64	4.58	0.50
Right frontal inferior gyrus, BA 46	296	36	34	6	4.40	0.48
Left cerebellum, posterior lobe	305	−32	−76	−22	4.12	0.45
Left parietal inferior lobule, BA 40	487	−55	−59	39	4.10	0.44
Left parietal inferior lobule, BA 40		−54	−50	46	3.79	0.41
Right parietal inferior lobule, BA 40	111	51	−43	50	4.07	0.44
Left parietal postcentral gyrus, BA 7	80	−9	−53	70	4.06	0.44
Right frontal superior gyrus, BA 9	269	4	58	28	4.00	0.43
Right frontal medial gyrus, BA 10		4	62	20	3.73	0.40
Left frontal middle gyrus, BA 9	304	−52	16	25	3.99	0.43
Left temporal middle gyrus, BA 21	44	−69	−10	−17	3.92	0.42
Left frontal superior gyrus, BA 10	62	−36	51	23	3.91	0.42
Left temporal superior gyrus, BA 22	294	−63	−55	22	3.88	0.42
Left temporal superior gyrus, BA 22		−63	−55	18	3.68	0.39
Right frontal rectal gyrus, BA 11	108	4	16	−26	3.88	0.42
Right frontal middle gyrus, BA 10	114	41	59	−10	3.83	0.41
Right temporal middle gyrus, BA 37	97	54	−58	−10	3.78	0.40
Left parietal superior lobule, BA 7	30	−18	−67	58	3.78	0.40
Right temporal middle gyrus, BA 21	83	73	−32	−14	3.74	0.40
Left frontal middle gyrus, BA 8	23	−34	38	41	3.68	0.39
Right temporal middle gyrus, BA 21	77	62	−49	7	3.68	0.39
Right frontal middle gyrus, BA 6	34	48	8	47	3.63	0.39
Right frontal superior gyrus, BA 8	19	26	23	51	3.60	0.38
White matter correlations with FSIQ						
Left frontal superior gyrus, BA 10	188	−20	64	−1	4.62	0.50
Right occipital cuneus, BA 18	338	4	−78	19	4.26	0.46
Left frontal inferior gyrus, BA 45	333	−31	29	9	4.23	0.46
Left frontal inferior gyrus, BA 47		−43	31	−13	4.02	0.43
Right parietal precuneus, BA 7	195	6	−60	46	4.06	0.44
Left temporal middle gyrus, BA 20	211	−57	−41	−8	4.04	0.44
Right temporal inferior gyrus, BA 21	25	58	−12	−18	3.81	0.41
Right temporal middle gyrus, BA 20	36	54	−39	−9	3.71	0.40
Left frontal precentral gyrus, BA 44	25	−51	9	12	3.70	0.39
Right temporal middle gyrus, BA 21	11	59	−35	−5	3.61	0.38

x, y, and z coordinates are in Talairach atlas space.
* $P < 0.05$ corrected for multiple comparisons.

Table 4
Number and size of voxel clusters with a significant correlation between gray matter and FSIQ for each brain lobe in the UNM and UCI samples[a]

	Frontal	Parietal	Temporal	Limbic	Occipital	Cerebellum	Total
UNM, No. of clusters	15	1	5	5	1	0	27
UNM, total voxels	22,846	251	14,901	3,022	283	0	41,303
Percentage of total	55.3%	.6%	36%	7.3%	.7%	0	
UCI, No. of clusters	13	6	6	0	0	1	26
UCI, total voxels	22,457	5,519	3,019	0	0	305	31,300
Percentage of total	71.7%	17.6%	9.6%	0	0	1%	

[a] These data are summarized from Tables 2 and 3; subclusters are not included in this summary.

two samples for the distribution across brain lobes of the major clusters of voxels with significant correlations between gray matter and FSIQ along with the total number of voxels in these clusters. Both samples show the most clusters and the highest number of voxels where GM and FSIQ are correlated ($P < 0.001$) to be in the frontal lobes, although the older UCI sample shows a higher portion of frontal lobe clusters than the younger UNM sample (71.7% versus 55.3%). The younger UNM sample has more clusters and voxels with a GM/FSIQ correlation in temporal and limbic lobes, and the older UCI sample has more in the parietal lobes. The total number of voxels in the UNM sample with a GM/FSIQ correlation ($P < 0.001$) is 41,303 and this represents 6.2% of all total gray matter voxels in the average UNM subject (660,870 total GM voxels). The total GM/FSIQ voxels in the older UCI sample is 31,300 or 5% of the total gray matter voxels in the average UCI subject (644,496 total GM voxels).

Discussion

These findings support the view that individual differences in gray and white matter volumes, in a relatively small number of areas distributed throughout the brain, account for considerable variance in individual differences in general intelligence. The locations of our strongest conjunction GM findings ($P < 0.05$, corrected for multiple comparisons) in the frontal lobes (BA 10, 46, and 9) are consistent with earlier functional imaging findings and reinforce the importance of frontal areas for general intelligence (Duncan et al., 2000; Gray et al., 2003; Haier et al., 1988). We also had similarly strong GM findings with posterior areas including BA 37,19, 40, and 43, which are consistent with earlier functional imaging findings identifying that activity in these areas was correlated to general intelligence (Duncan et al., 2000; Gray et al., 2003; Haier et al., 1988, 2003b). Interestingly, in the younger UMN sample, the strongest GM/FSIQ correlation was in left temporal lobe, BA 37 (see Haier et al., 2003b).

These results expand upon recent research relating IQ to gray matter in a normal pediatric population using VBM (Wilke et al., 2003). These authors found gray matter within the anterior cingulate to be most associated with performance on the Wechsler Intelligence Scale for Children—III, with the older children (mean age = 15.4 ± 1.86 years) accounting for the bulk of the effect. It is of note that our young group (mean age = 27 ± 5.9 years) displayed numerous correlations at $P < 0.001$ within medial frontal gray and white matter regions adjacent to the anterior cingulate cortex. Taken together, the relationship between frontal brain regions and IQ across different ages appears to progress from anterior cingulate (pediatric cohort), to medial frontal (young UNM cohort), to more dorsolateral frontal regions (older UCI cohort). We suspect that the progression observed across these cohorts is likely modulated by accelerated brain volume loss across the life span preferentially affecting frontal gray matter (Raz et al., 1997), particularly the anterior cingulate gyrus (Good et al., 2001). Our interpretation of these data is limited because different MRI scanners were used between samples.

Although correlation data do not speak to why some individuals have more gray matter in some areas than other individuals, GM in many of the areas identified here show high heritability (Thompson et al., 2001). Our data support the view that most of the heritable portion of *g* variance can be accounted for by GM in frontal areas (Thompson et al., 2001), and our data also show that additional portions of significant *g* variance can be accounted for by GM in posterior areas.

Whole brain white matter may be more correlated to intelligence than whole brain gray matter (Gignac et al., 2003), but there is little data on regional white matter correlates of intelligence. Our main WM findings are mostly adjacent to our GM findings and may represent relatively fine interlacing of GM and WM not easily differentiated with the VBM technique. Alternatively, the white matter areas, which show correlations with general intelligence, may also represent pathways independent of GM that underlie general intelligence. For example, MRI spectroscopy indicates that a neurometabolite (*N*-acetylaspartate, NAA) in WM in the left occipitoparietal area is correlated to general intelligence in normal subjects (Jung et al., 1999a,b) and may indicate more myelin and the facilitation of neural transmission in this area. Possibly consistent with this, our strongest WM finding ($P < 0.05$, corrected) was in the right parietal area closest to BA 39, contiguous with the spectroscopic voxel of interest. Thus, brain volume–IQ correlations are not likely to be exhaustive and may be constrained by metabolic integrity at the level of the neuron–axon.

These observations lead us to hypothesize that more white matter in this area near BA 39 may facilitate the transmission of sensory information from numerous posterior areas to the frontal lobes, where more gray matter results in better processing that manifests as higher intelligence scores. Larger sample multivariate studies can clarify which areas work together and account for most *g* variance and studies of groups with impaired regional GM may help determine whether frontal GM is necessary or sufficient for obtaining high *g* scores. As indicated in Table 1 and Fig. 2, younger adults may show different patterns than older adults, likely reflecting the cumulative effects of neuronal loss over time.

The finding that gray and white matter volumes in a number of areas similarly account for considerable variance in general intelligence suggests a basis for why people of the same IQ often show different cognitive strengths and weaknesses. Structural brain differences in gray and white matter volumes in specific areas may, to some extent, determine the pattern of functional correla-

tions in imaging studies of intelligence independently of task demands. For any individual, the pattern of GM and WM volumes in relevant areas may constrain which areas work together and are activated or deactivated during problem solving, reasoning, or even passive information processing. Similar task performance may be attained if different combinations of brain areas provide independent pathways for good performance. This would also suggest a basis for the observation that regional brain damage from head injury or stroke often does not decrease IQ. These data also suggest that it may be possible to assess individual differences in mental ability using multivariate combinations of gray and white matter volumes from a relatively small number of brain regions easily assessed using structural MRIs.

Having more gray matter in an area available for processing may also account for the inverse correlations reported in several studies between brain activation and good performance on *g*-loaded tasks (Haier et al., 1988; Parks et al., 1988), provided that more gray matter results in less energy use when that area is employed (efficiently) for specific cognitive tasks. Although inverse correlations have been reported between brain size and cerebral glucose metabolic rate (Haier et al., 1995; Hatazawa et al., 1987; Yoshii et al., 1988), additional study is needed of regional correlations between cerebral structure and function.

Finally, we note the relatively small proportion of distributed gray matter voxels correlated to FSIQ in both samples. This suggests that the integration of the constant flow of information moving throughout the brain that is important to intelligent behavior may well be accomplished with an efficient use of relatively few and finite structures. We are reminded by one of the founding fathers of neuroscience, A.R. Luria, that complex behaviors are "organized in systems of concertedly working zones, each of which performs its role in complex functional system, and which may be located in completely different and often far distant areas of the brain" (Luria, 1973, p. 31). Our research highlights the "dynamic localization" of intellectual processes across the life span and suggests a critical interplay of discrete frontal and posterior brain regions.

Acknowledgment

The UCI portion of this work was funded by a grant from NICHD to Dr. Haier (HD037427).

References

Ashburner, J., Friston, K.J. 2000. Voxel-based morphometry—The methods. NeuroImage 11 (6 Pt 1), 805–821.

Ashburner, J., Friston, K.J. 2001. Why voxel-based morphometry should be used. NeuroImage 14 (6), 1238–1243.

Boivin, M.J., Giordani, B., Berent, S., et al., 1992. Verbal fluency and positron emission tomographic mapping of regional cerebral glucose-metabolism. Cortex 28 (2), 231–239.

Duncan, J., Seitz, R.J., Kolodny, J., et al., 2000. A neural basis for general intelligence. Science 289 (5478), 457–460.

Flashman, L.A., Andreasen, N.C., Flaum, M., et al., 1997. Intelligence and regional brain volumes in normal controls. Intelligence 25 (3), 149–160.

Gignac, G., Vernon, P.A., Wickett, J.C., 2003. Factors influencing the relationship between brain size and intelligence. The Scientific Study of general Intelligence. H. Nyborg, Pergamon, Amsterdam, pp. 93–106.

Good, C.D., Johnsrude, I.S., Ashburner, J., et al., 2001. A voxel-based morphometric study of ageing in 465 normal adult human brains. NeuroImage 14 (1 Pt 1), 21–36.

Good, C.D., Scahill, R.I., Fox, N.C., et al., 2002. Automatic differentiation of anatomical patterns in the human brain: validation with studies of degenerative dementias. NeuroImage 17 (1), 29–46.

Gray, J.R., Chabris, C.F., Braver, T.S., 2003. Neural mechanisms of general fluid intelligence. Nat. Neurosci. 6 (3), 316–322.

Haier, R.J., Benbow, C.P., 1995. Sex differences and lateralization in temporal lobe glucose metabolism during mathematical reasoning. Dev. Neuropsychol. 11 (4), 405–414.

Haier, R.J., Siegel, B.V., Nuechterlein, K.H., et al., 1988. Cortical glucose metabolic rate correlates of abstract reasoning and attention studied with positron emission tomography. Intelligence 12 (2), 199–217.

Haier, R.J., Siegel, B.V. Jr., MacLachlan, A., et al., 1992a. Regional glucose metabolic changes after learning a complex visuospatial/motor task: a positron emission tomographic study. Brain Res. 570 (1–2), 134–143.

Haier, R.J., Siegel, B.V., Tang, C., et al., 1992b. Intelligence and changes in regional cerebral glucose metabolic rate following learning. Intelligence 16 (3–4), 415–426.

Haier, R.J., Chueh, D., Touchette, P., et al., 1995. Brain size and cerebral glucose metabolic rate in nonspecific mental retardation and Down syndrome. Intelligence 20 (2), 191–210.

Haier, R.J., Alkire, M.T., White, N.S., et al., 2003a. Temporal cortex hypermetabolism in Down syndrome prior to the onset of dementia. Neurology 61 (12), 1673–1679.

Haier, R.J., White, N.S., Alkire, M.T., 2003b. Individual differences in general intelligence correlate with brain function during nonreasoning tasks. Intelligence 31 (5), 429–441.

Hatazawa, J., Brooks, R.A., Di Chiro, G., et al., 1987. Glucose utilization rate versus brain size in humans. Neurology 37 (4), 583–588.

Jensen, A. 1980. Bias in Mental Testing Free Press, New York.

Jung, R.E., Brooks, W.M., Yeo, R.A., et al., 1999a. Biochemical markers of intelligence: a proton MR spectroscopy study of normal human brain. Proceedings of the Royal Society of London Series B-Biological Sciences 266 (1426), 1375–1379.

Jung, R.E., Yeo, R.A., Chiulli, S.J., et al., 1999b. Biochemical markers of cognition: a proton MR spectroscopy study of normal human brain. NeuroReport 10 (16), 3327–3331.

Luria, A.R., 1973. The Working Brain: An Introduction to Neuropsychology. Penguin Press, London.

MacLullich, A.M.J., Ferguson, K.J., Deary, I.J., et al., 2002. Intracranial capacity and brain volumes are associated with cognition in healthy elderly men. Neurology 59 (2), 169–174.

Parks, R.W., Loewenstein, D.A., Dodrill, K.L., et al., 1988. Cerebral metabolic effects of a verbal fluency test—A Pet Scan Study. J. Clin. Exp. Neuropsychol. 10 (5), 565–575.

Prabhakaran, V., Smith, J.A., Desmond, J.E., et al., 1997. Neural substrates of fluid reasoning: an fMRI study of neocortical activation during performance of the Raven's Progressive Matrices Test. Cogn. Psychol. 33 (1), 43–63.

Price, C.J., Friston, K.J., 1997. Cognitive conjunction: a new approach to brain activation experiments. NeuroImage 5 (4 Pt. 1), 261–270.

Raz, N., Gunning, F.M., Head, D., et al., 1997. Selective aging of the human cerebral cortex observed in vivo: differential vulnerability of the prefrontal gray matter. Cereb. Cortex 7 (3), 268–282.

Spearman, C., 1904. General intelligence objectively determined and measured. Am. J. Psychol. 15, 201–293.

Talairach J., Tournoux P., 1988. Co-planar stereotaxic atlas of the human brain: a 3-dimensional proportional system, an approach to cerebral imaging, G. Thieme, Stuttgart; Thieme Medical Publishers, New York.

Thompson, P.M., Cannon, T.D., Narr, K.L., et al., 2001. Genetic influences on brain structure. Nat. Neurosci. 4 (12), 1253–1258.

Wechsler, D., 1981. Wechsler Adult Intelligence Scale—Revised. Psychologica Corporation, San Antonio, TX.

White, N.B., Alkire, M.T., Haier, R.J., 2003. A voxel-based morphometric study of non-demented adults with Down syndrome. NeuroImage 20 (1), 393–403.

Wilke, M., Sohn, J.H., Byars, A.W., et al., 2003. Bright spots: correlations of gray matter volume with IQ in a normal pediatric population. NeuroImage 20 (1), 202–215.

Yoshii, F., Barker, W.W., Chang, J.Y., et al., 1988. Sensitivity of cerebral glucose metabolism to age, gender, brain volume, brain atrophy, and cerebrovascular risk factors. J. Cereb. Blood Flow Metab. 8 (5), 654–661.